Author's Accepted Manuscript

www.elsevier.com/locate/talanta

Ultrasensitive aptamer biosensor for arsenic (III) detection based on label-free triple-helix molecular switch and fluorescence sensing platform

Jiafeng Pan, Qiong Li, Danhua Zhou, Junhua Chen

PII: S0039-9140(18)30716-1
DOI: https://doi.org/10.1016/j.talanta.2018.07.024
Reference: TAL18853

To appear in: *Talanta*

Received date: 2 April 2018
Revised date: 25 June 2018
Accepted date: 10 July 2018

Cite this article as: Jiafeng Pan, Qiong Li, Danhua Zhou and Junhua Chen, Ultrasensitive aptamer biosensor for arsenic (III) detection based on label-free triple-helix molecular switch and fluorescence sensing platform, *Talanta,* https://doi.org/10.1016/j.talanta.2018.07.024

Ultrasensitive aptamer biosensor for arsenic (III) detection based on label-free triple-helix molecular switch and fluorescence sensing platform

Jiafeng Pan[a], Qiong Li[a,b], Danhua Zhou[a,c], Junhua Chen[a,*]

[a]Guangdong Key Laboratory of Integrated Agro-environmental Pollution Control and Management, Guangdong Institute of Eco-environmental Science & Technology, Guangzhou, 510650, China.

[b]College of Bioscience and Biotechnology, Hunan Agricultural University, Changsha, 410128, China.

[c]College of Natural Resources and Environment, South China Agricultural University, Guangzhou, 510642, China.

[*]Corresponding author: 222chenjunhua@163.com

Abstract

Arsenic ion is a well-known harmful heavy element widely existing in the environment. Arsenic pollution occurring frequently has become increasing a serious worldwide threat to human health and the environment. The development of sensitive and reliable methods to detect As^{3+} in water is of great importance to biochemical research and monitoring applications. Herein, a label-free fluorescence sensing platform was elaborately designed for As^{3+} monitoring using exonuclease III (Exo III)-assisted cascade target recycling amplification strategy. The triple-helix molecular switch was employed as the sensing element and 2-amino-5,6,7-trimethyl-1,8-naphthyridine was used as the signal indicator. The resulting biosensor is simple, ultrasensitive, and exhibits a limit of detection of 5 ng/L with high selectivity. Meanwhile, the proposed sensor is successfully applied to determination of As^{3+} in practical sample analysis (tap water, lake water and pond water). The results shown herein have important implications in the development of new fluorescent sensors for the fast, easy, and selective detection and quantification of As^{3+} in water samples. More importantly, the proposed platform can be extended to detect other heavy metal ions with newly designed triple-helix molecular switch, as well as pesticide residue, antibiotic residues, and biomarkers by using aptamer sequences.

Graphical Abstract:

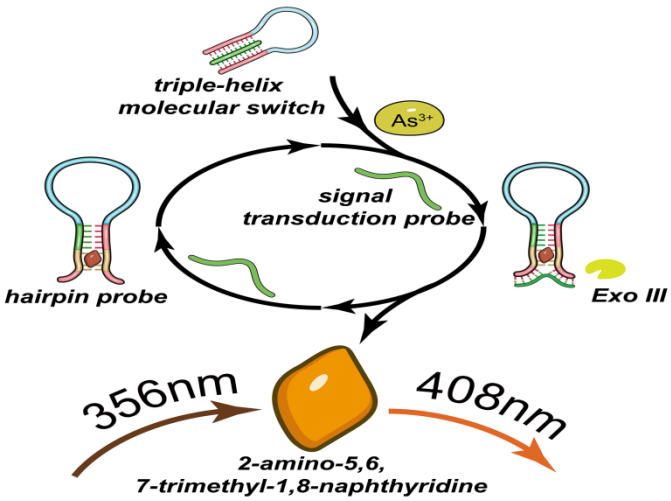

Keywords: Label-free; Exonuclease III-assisted signal amplification; Triple-helix molecular switch; 2-amino-5,6,7-trimethyl-1,8-naphthyridine; Aptamer biosensor.

1. Introduction

Arsenic ion (As^{3+}) is a well-known harmful heavy element widely existing in the environment [1]. Arsenic pollution occurring frequently has become increasing a serious worldwide threat to human health and the environment [2]. It is estimated that arsenic contamination levels have been much higher than 10 ppb in many countries and regions in drinking water, which was set as the maximum contaminant level (MCL) of total arsenic by the U.S. Environmental Protection Agency (EPA) [3]. The development of sensitive and reliable methods to detect As^{3+} in water is of great importance to biochemical research and monitoring applications. Several reliable methods have been reported for detection for As^{3+}, such as high performance liquid chromatography (HPLC) [4], atomic absorption spectroscopy (AAS) [5], and atomic fluorescence spectroscopy (AFS) [6]. Although these analytical techniques are sensitive and accurate, most of them necessitate the use of costly apparatus and require complicated pretreatment procedures and so are inappropriate for on-site and real-time detection. To overcome their drawback, researchers are now shifting to low cost and rapid sensing strategies [7]. Despite the development of ultrasensitive As^{3+} biosensor has become a growing attention in last decade [8,9], most of them usually needed complicated instrumentation, thus limiting their wide applications. Therefore, it is highly desirable to develop a fast, sensitive, and cost-effective method for As^{3+} detection.

Recently, an aptamer for As^{3+} was selected by SELEX, which shows excellent specificity because of its unique structures [10]. Since then, several related researches have been reported on the aptasensors for As^{3+} utilizing different signal transduction strategies such as colorimetry [11-13], electrochemical [14,15], or fluorescence [16,17]. Among these aptasensors, fluorescence aptasensors have witnessed very rapid development due to the advantages of high sensitivity, impressive specificity, simplicity and quick respond. Owing to the conformational alteration of the aptamer during the binding event between aptamer and target, various DNA molecular switches have been designed for constructing convenient aptamer-based fluorescent sensing strategies, such as double-helix DNA molecular switches [18], molecular beacon [19], and newly reported triple-helix molecular switch (THMS) [20]. However, the researches of THMS are rare for other small molecules or ions [21]. So it is great significant to explore the universality of the THMS sensing strategy for more low-weight targets.

Herein, a label-free fluorescence sensing platform was elaborately designed for As^{3+}

monitoring using Exo III-assisted cascade target recycling amplification strategy. The THMS was employed as the sensing element and 2-amino-5,6,7-trimethyl-1,8-naphthyridine (ATMND) was used as the signal indicator. The integration of THMS, Exo III and ATMND may pave a novel and cost-effective way toward As^{3+} monitoring. The proposed method could selectively detect As^{3+} down to 5 ng/L. The fluorescence sensor also has high selectivity toward As^{3+} in the presence of other competitive molecules. The biosensor is robust and has been successfully applied to As^{3+} detection in tap water, lake water, and river water samples.

2. Materials and methods

2.1 Reagents and materials

Exo III was purchased from Takara (Dalian, China) and used without further purification. ATMND was obtained from Enamine (Ukraine). SYBR Green was bought from Thermo Fisher Scientific Co. (Shanghai, China). TBE-urea sample buffer was obtained from Bio-Rad Co. Boric acid, ethylenedinitrilotetraacetic acid disodiumsalt (EDTA-2Na), urea, acrylamide, Tris (hydroxymethyl) aminomethane (Tris), ammonium persulfate (APS), N,N′-methylenebisacrylamide, N,N,N′,N′-tetramethylethylenediamine (TEMED), $MgCl_2$ and NaCl were provided by J & K Scientific Ltd. (China). As^{3+} and its competitive metal ions, including As^{5+}, Pb^{2+}, Cd^{2+}, Ag^{+}, Mg^{2+}, Zn^{2+}, Mn^{2+}, Ni^{2+} and Cu^{2+} were produced by Sigma-Aldrich (USA). Tetracycline (TE) and methyl parathion (MP) were from Huaerbo Chemical Reagent Co. All the other chemicals were of analytical grade and ultrapure water (Milli-Q18.2 MΩ, Millipore System Inc.) was used for all the experiments. All the ULTRAPGE-purified oligonucleotides were synthesized by Sangon Biological Engineering Technology & Co. Ltd. (Shanghai, China) and the sequences are listed as follows.

STP: 5′-GAGAGAGAGATTAAAT-3′

ABA1: 5′-CTCTCTCTTACAGA ACAACCAACGTCGCTCCGGGTACTTCTTCATCGCTCTCTC-3′

ABA2: 5′-CTCTCTCTTTACAGAACAAC CAACGTCGCTCCGGGTACTTCTTCATCGTCTCTCTC-3′

ABA 3: 5′-CTCTCTCTCTTACAGAACAACCAA CGTCGCTCCGGGTACTTCTTCATCGCTCTCTCTC-3′

ABA4: 5′-CTCTCTCTCTTTACAGAACAACCAAC GTCGCTCCGGGTACTTCTTCATCGTCTCTCTCTC-3′

HP1: 5′-TCTCCGCCGAGAGAGAGATCCAATCA CAACTCTCTCTCTCGCCGTCTCTC-3′

2.2 Apparatus

The fluorescence excitation and emission spectra were recorded on the F-7000 Fluorescence Spectrophotometer (Japan) during the whole experiments. The polyacrylamide gel electrophoresis (PAGE) experiments were performed by a DYY-8C electrophoresis instrument and a DYCZ-24A vertical electrophoresis tank (Liuyi Instrument Factory, Beijing, China).

2.3 As^{3+} detection procedure

Firstly, THMS was formed by pre-hybridization of the aptamer sequence flanked by two arm segments with STP on the basis of Watson-Crick and Hoogsteen base pairings. In our experiences, the conserved region of the aptamer is the vital binding site for the ligand. The aptamer can be tailored to design various biosensors as long as keeping the conserved domains intact. 10 μL of 100 μM STP (with the final concentration of 10 μM) and 10 μL of 100 μM aptamer flanked by two arm segments (with the final concentration of 10 μM) were mixed in 80 μL of 20 mM Tris buffer solution (pH 7.6) that contained 7 mM of $MgCl_2$ and 95 mM of NaCl for the assembling of THMS, followed by incubation at 37 ^{o}C for 20 min to thoroughly hybridize them with each other. Subsequently, the HP1 and ATMND with stoichiometric ratio of 1:1 were mixed, heated to 95 °C for 7 min, and then cooled down to room temperature to form a stable ATMND/HP1 complex.

For As^{3+} detection, 20 μL of the As^{3+} solution containing 50 U Exo III was added into 180 μL Tris-HCl buffer solution that contained 1 μM THMS and 1 μM ATMND/HP1 complex. The mixture was kept for 30 min to complete the reaction. After the activity of Exo III was denatured, the fluorescence spectra of the system was recorded at an excitation wavelength of 356 nm.

2.4 Polyacrylamide gel electrophoresis analysis

A 12% denatured PAGE gel was used to perform the electrophoresis analysis, which was prepared by mixing 5 mL of 30% Acr-Bis solution (29:1), 1 mL of 10×TBE buffer solution, 100 μL of APS (10%), 4 μL of TEMED and 3.8 mL of ultrapure water, and followed with polymerized at room temperature for 90 min. The electrophoresis experiments were carried out in the running buffer of 1×TBE, at a constant voltage of 70 V for 90 min, with the loading of 5 μL of DNA sample including a loading buffer (V/V, 1:5). After staining in diluted SYBR gold solution, the PAGE gels

were photographed in a Gel Doc XR system (Bio-Rad).

3. Results and discussion

3.1 Principle of the label-free fluorescence sensing platform

The principle of the label-free fluorescence sensing platform for As^{3+} detection is illustrated in Scheme 1. Typically, the THMS includes the label-free signal transduction probe (STP) and target specific hairpin-shaped aptamer sequence as the central with two arm segments. The fluorescent small molecule ATMND can selectively bind to a cytosine (C) at a C–C mismatch in double-stranded DNA with high affinity via the strong π-π stacking interaction. A hairpin probe (HP1) has been elaborately designed of the assay with three functional sections, which contains a C-C mismatch in the stem in order to forming the ATMND/HP1 complex [22], two protruding oligonucleotide segments at both the 3' and 5' ends to recognize the STP, and a secondary target analogue caged in the stem for further signal amplification. Exo III is applied for recycling both the initial and the secondary STP, as well as to successively releasing the ATMND for signal reporting. The reason of selecting Exo III as a signal amplification unit is because it is a sequence independent enzyme which could provide a versatile platform for amplified detection of As^{3+} at room temperature [23-25]. In the absence of As^{3+}, the THMS is turn-off and the STP is locked, and Exo III could not digest the ATMND/HP1 complex with more than 4 bases overhang at its 3-terminus [26,27], so the ATMND/HP1 complex is very stable and demonstrates a low fluorescence background. Upon the addition of As^{3+}, the THMS is turn-on that the aptamer sequence is bind to As^{3+} producing the free STP, then the hybridization between STP and ATMND/HP1 triggers the Exo III's digestion, coupled with the release of the STP, a secondary STP analogue and ATMND. The released initial and the secondary STP analogue both recycle and hybridize with other complex to begin the cycle anew, thus generating a great amount of free ATMND with high fluorescence in succession. Based on the change of the fluorescence intensity, the highly sensitive detection of As^{3+} can be realized.

3.2 Feasibility of the label-free fluorescence sensing platform

To explore the viability of the label-free and fluorescence sensing platform, the fluorescence spectra of the As (III) sensor at different conditions were recorded and shown in Fig. 1A. Due to the high fluorescence quantum yield [28,29], under the excitation of 356 nm, the free THMS

showed a low fluorescence emission peak at 408 nm (curve g, Fig. 1A). And the free ATMND showed a strong fluorescence emission peak at 408 nm (curve a). Addition of HP1 to the ATMND solution led to a significant decrease in the fluorescence intensity (curve d). This phenomenon was consistent with the previous reports that the ATMND could be trapped by the C-C mismatch with high affinity and quenched by the bases flanking the mismatch via the strong π-π stacking interaction [30], thus indicating the formation of the ATMND/HP1 complex. Addition of THMS and the ATMND/HP1 complex led to a slight decrease in the fluorescence intensity (curve f), which is as same as the intensity of adding As^{3+} (curve e). In the presence of the As^{3+}, which contained both the As^{3+} and Exo III, the fluorescence intensity of ATMND significantly increased (curve b). These results indicated the significant signal enhancement in curve b was due to the synergistic interaction. Firstly, the aptamer coupled to As^{3+} led to the STP released. Subsequently, the hybridization between the STP and the ATMND/HP1 complex triggered the exonuclease activity of Exo III, which rapidly catalyzed the step removal of 3′-mononucleotides from the ATMND/HP1 complex, recycled the STP and the secondary STP analogous, and simultaneously recovered the fluorescence of ATMND with high amplification times. Correspondingly, based on the obvious fluorescence signal enhancement, the concentration of As^{3+} could be detected.

As shown in Fig. 1B, the six lanes in the PAGE image corresponded to the ATMND/HP1 (Lane a), THMS+ATMND/HP1 (Lane b), THMS+ATMND/HP1+Exo III (Lane c), THMS+ATMND/HP1+As^{3+}+Exo III (Lane d), THMS +ATMND/HP1+As^{3+} (Lane e), and THMS (Lane f), respectively. Obviously, a band corresponded to THMS and ATMND/HP1 were observed in lane f and a. Upon the addition of the metal ions solution which was absent of As^{3+}, the ATMND/HP1 was slightly digested by Exo III, which was reflected by the emergence of a new band under that of the ATMND/HP1 (Lane c). This phenomenon was constant with the fluorescence spectrum of curve c in Figure 1A, indicating the nonspecific digestion process would result in a slight enhancement in the background signal [31-34]. However, almost no ATMND/HP1 could be observed in lance d, indicating the simultaneous addition of As^{3+} and Exo III could trigger the enzymatic activity of Exo III to completely digest all of ATMND/HP1 and effciently release ATMND for signal amplification. These results are further verified the feasibility of the proposed strategy.

3.3 Optimization of experimental conditions

The molar ratio of HP1 to ATMND that affects the sensitivity of the biosensor was optimized. Using a fixed concentration (1 μM) of HP1, the effect of molar ratio of HP1 to ATMND on the response of the biosensor was first evaluated by detecting 1 mg/L As^{3+}. As shown in Fig. 2, the signal-to-noise (S/N) ratio increased with the increment of the molar ratio of HP1 to ATMND from 1:1 to 6:1, further increasing the molar ratio caused a decrease of the S/N ratio. The reason for this result is that too much ATMND cause a high background signal, while deficient amount of ATMND would result in a weak fluorescence signal. Therefore, the molar ratio of HP1 to ATMND of 6:1 was used for As^{3+} detection to achieve the best signal-to-noise level.

It had been noted that the stem length of the THMS structure plays an important role in the sensor performance. The As^{3+} aptamer was extended at the 3'- and 5'- ends with two arm segments. The effect of the stem lengths on the formation of THMS was evaluate by varying the DNA sequences of the arm segments from 7 to 10 bases. (ABA1 flanked by the 7 bases arm segments, ABA2 flanked by the 8 bases arm segments, ABA3 flanked by 9 the bases arm segments, and ABA4 flanked by 10 the bases arm segments, respectively). As shown in Fig. 3, by increasing the stem length from 7 to 10 bases, the fluorescence intensity decreased accordingly. Thus, ABA1 flanked by 7 bases arm segments was optimal for further experiments.

The concentration of ABA1 is also an important factor that influences the THMS formation. Hence, the influences of different concentration of ABA1 on the formation of THMS were carefully evaluated. Increasing concentrations of ABA1 (1, 2, 3, and 4 μM) were added to a constant concentration of STP (1 μM) in 200 μL Tris-HCl buffer solution, followed by incubation at 37 ^{o}C for 20 min for the assembling of THMS. Then the fluorescence spectra were recorded at room temperature. As shown in Fig. 4, the maximum S/N ratio was obtained with the concentration of ABA1 at 2 μM. The reason might be attributed to the fact that too much ABA1 would induce an insufficient THMS between ABA1 and STP, thus yielding a weak signal, while deficient amount of ABA1 would result in unstable THMS and cause a high background signal. Therefore, 2 μM ABA1 was chosen as the optimal concentration.

Meanwhile, the incubation time is another factors involved in DNA interactions, so the parameter was optimized to achieve the optimal detection efficiency. According to the

experimental results (Fig. 5), the fluorescence intensity increased gradually with increasing incubation time and reached a plateau after 30 min, indicating that the ATMND/HP1 complex had been fully digested and released the ATMND. Herein, 30 min was employed as the optimum incubation time for the sensing platform.

3.4 Detection performance

To assess the detection range and sensitivity of the proposed platform, different concentrations of As^{3+} have been analyzed under those optimized conditions. As shown in Fig. 6A, the responsive fluorescence emission spectra (fluorescence intensity at 408 nm, F_{408}) gradually grows along with As^{3+} concentration. F_{408} exhibits a linear growth with a correlation coefficient of 0.98 (Fig. 6B), upon plotting against the logarithm of As^{3+} concentrations. This relationship is well-described by the regression equation of F_{408}=90.68+9.14 lgC, where F_{408} is the fluorescence intensity at 408 nm. And C is the As^{3+} concentrations in the range of 10 ng/L to 10 mg/L. On the basis of three times the standard deviation of the blank measurement, detection limit of the proposed method has been calculated to be 5 ng/L. The LOD is significantly lower than that of reported methods based on fibre-optic (the LODs was 18 μg/L) [35], colorimetry (the LODs was 5.3 μg/L) [13], voltammetric (the LODs was 2.5 μg/L) [36], electrochemical (the LODs was 0.94 μg/L) [14], fluorescence (the LODs was 0.2 μg/L) [17], which demonstrates the ultrasensitivity of the proposed sensing platform.

3.5 Selectivity and practical sample analysis

The selectivity of the constructed biosensor is examined by monitoring fluorescence change of the solution with the presence of As^{3+} against other control molecules, including As^{5+}, Ag^{+}, Cd^{2+}, Cu^{2+}, Mg^{2+}, Mn^{2+}, Ni^{2+}, Pb^{2+}, Zn^{2+}, tetracycline (TE), and methyl parathion (MP). As shown in Fig. 7, the fluorescence intensity of As^{3+}, As^{5+}, Ag^{+}, Cd^{2+}, Cu^{2+}, Mg^{2+}, Mn^{2+}, Ni^{2+}, Pb^{2+}, Zn^{2+}, TE, and MP could recover 37.2, 6.1, 5.7, 4.9, 3.8, 2.4, 5.2, 3.7, 2.5, 2.9, 2.3, 2.35, respectively. The results demonstrate that our developed sensor exhibits a high selectivity to As^{3+} over other competing molecules.

The practical application of the label-free fluorescence sensing platform was evaluated by a recovery experiment performed in groundwater spiked with different concentrations of As^{3+}. The

As^{3+} spiked samples were then carried out for fluorescence analysis according to the operation procedures in the Tris-HCl buffer solution. As shown in Table 1, the recoveries of the spiked samples were in the range of 97-110.5 %, which indicated that the possible interference from practical water samples was negligible in the present system. Moreover, the proposed method was further tested with several other water samples including tap water, lake water, and pond water. Those water samples were analyzed separately using the fluorescence sensor and conventional liquid chromatography-tandem mass spectrometry (LC-MS/MS). The results of the As^{3+} determination in real water samples were summarized in Table 2. The data revealed that no significant difference existed between the values measured using the proposed biosensor and LC-MS/MS method, confirming the accuracy of the developed sensor for detecting As^{3+}. The above results showed that the as-proposed platform can be applied to the analysis of As^{3+} in real samples.

4. Conclusions

In summary, a simple and label-free fluorescence sensing platform based on ATMND/HP1-mediated THMS and the Exo III-assisted signal amplification has been successfully proposed for the ultrasensitive detection of As^{3+}. Under optimal conditions, the sensing platform showed a wide linear range from 10 ng/L to 10 mg/L and a LOD of 5 ng/L with high selectivity. The operation is simple, just need to mix these nucleic acids and Exo III for As^{3+} detection. Our proposed sensor described herein is simple in operation without labeling and immobilization procedures or separation and washing steps. Also, the sensing platform is fast (each test needs about 30 min) and cost-effective (each test costs approximately $ 0.67 U.S. dollars). In particular, the proposed platform can be extended to detect other heavy metal ions with newly designed THMS, as well as pesticide residue, antibiotic residues, and biomarkers by using aptamer sequences. Practical sample analysis demonstrated the method had good precision and accuracy, thus indicating its great application potentials for detection of As^{3+} in complex water samples.

Acknowledgements

Financial support was provided by the Guangdong Natural Science Funds for distinguished Young Scholar (2016A030306012), the Special Support Program for Young

Talent Scholar of Guangdong Province (2015TQ01Z092), the GDAS' Special Project of Science and Technology Development (2017GDASCX-0405), the Science and Technology Program of Guangdong Province (2016B070701015, 2016B020204003), and the SPICC Program (2016GDASPT-0105).

References

[1] H. Kaur, R. Kumar, J.N. Babu, S. Mittal, Advances in arsenic biosensor development-A comprehensive review, Biosens. Bioelectron. 63 (2015) 533-545.

[2] S. Kempahanumakkagari, A. Deep, K.H. Kim, K.S. Kumar, H.O. Yoon, Nanomaterial-based electrochemical sensors for arsenic-A review, Biosens. Bioelectron. 95 (2017) 106-116.

[3] G. Aragay, J. Pons, A. Merkoci, Recent trends in Macro-, Micro-, and nanomaterial-based tools and strategies for heavy-metal detection, Chem. Rev. 111 (2011) 3433-3458.

[4] A.H. Ackerman, P.A. Creed, A.N. Parks, M.W. Fricke, C.A. Schwegel, J.T. Creed, D.T. Heitkemper, N.P. Vela, Comparison of achemical and enzymatic extraction of arsenic from rice and an assessment of the arsenic absorption from contaminated water by cooked rice, Environ. Sci. Technol. 39 (2005) 5241-5246.

[5] M. Jakariya, M. Vahter, M. Rahman, M.A. Wahed, S.K. Hore, P. Bhattacharya, G. Jacks, L. ÅkePersson, Screening of arsenic in tubewell water with field test kits: Evaluation of the method from public health perspective, Sci. Total. Environ. 379 (2007) 167-175.

[6] D. Fang, R. Dong, Y. Kai, X. Luo, X. Tu, S. Luo, L. Yang, Determination of trace total inorganic arsenic by hydride generation atomic fluorescence spectrometry after solid phase extraction-preconcentration on aluminiumhydroxide gel, Mikrochim. Acta. 180 (2013) 509-515.

[7] P. Weerathunge, R. Ramanathan, R. Shukla, T.K. Sharma, V. Bansal, Aptamer-controlled reversible inhibition of gold nanozyme activity for pesticide sensing, Anal. Chem. 86 (2014) 11937-11941.

[8] K. Morita, E. Kaneko, Spectrophotometric determination of trace arsenic in water samples using a nanoparticle of ethyl violet with a molybdate-iodine tetrachloride complex as a probe for molybdoarsenate, Anal. Chem. 78 (2006) 7682-7688.

[9] M. Mulvihill, A. Tao, K. Benjauthrit, J. Arnold, P. Yang, Surface-enhanced raman spectroscopy

for trace arsenic detection in contaminated water, Angew. Chem. Int. Ed. 120 (2008) 6456-6460.

[10] M. Kim, H.J. Um, S. Bang, S.H. Lee, S.J. Oh, J.H. Han, K.W. Kim, J. Min, Y.H. Kim, Arsenic removal from vietnamese groundwater using the arsenic-binding DNA aptamer, Environ. Sci. Technol. 43 (2009) 9335-9340.

[11] K. Chauhan, P. Singh, B. Kumari, R.K. Singhal, Synthesis of new benzothiazole schiffbase as selective and sensitive colorimetric sensor for arsenic on-site detection at ppb level, Anal. Chem. 9 (2017) 1779-1785.

[12] A. Gupta, N.C. Verma, S. Khan, C.K. Nandi, Carbon dots for naked eye colorimetric ultrasensitive arsenic and glutathione detection, Biosens. Bioelectron. 81 (2016) 465-472.

[13] Y. Wu, S. Zhan, F. Wang, L. He, W. Zhi, P. Zhou, Cationic polymers and aptamers mediated aggregation of gold nanoparticles for the colorimetric detection of arsenic(III) in aqueous solution, Chem. Commun. 48 (2012) 4459-4461.

[14] F. Cortéssalazar, S. Beggah, V.D.M. Jr, H.H. Girault, Electrochemical As(III) whole-cell based biochip sensor, Biosens. Bioelectron. 47 (2013) 237-242.

[15] L. Cui, J. Wu, H. Ju, Label-Free signal-on aptasensor for sensitive electrochemical detection of arsenite, Biosens. Bioelectron. 79 (2016) 861-865.

[16] A.A. Ensafi, N. Kazemifard, B. Rezaei, A simple and sensitive fluorimetricaptasensor for the ultrasensitive detection of arsenic (III) based on cysteaminestabilized CdTe/ZnSquantum dots aggregation, Biosens. Bioelectron. 77 (2016) 499-504.

[17] L. Zhang, X. Cheng, L. Kuang, A. Z. Xu, R.P. Liang, J.D. Qiu, Simple and highly selective detection of arsenite based on the assembly-induced fluorescence enhancement of DNA quantum dots, Biosens. Bioelectron. 94 (2017) 701-706.

[18] N. Li, C.M. Ho, Aptamer-based optical probes with separated molecular recognition and signal transduction modules, J. Am. Chem. Soc. 130 (2008) 2380-2381.

[19] X. Wang, P. Dong, W. Yun, Y. Xu, P. He, Y. Fang, A solid-state electrochemiluminescence biosensing switch for detection of thrombin based on ferrocene-labeled molecular beacon aptamer, Biosens. Bioelectron. 24 (2009) 3288-3292.

[20] J. Zheng, J. Li, Y. Jiang, J. Jin, K. Wang, R. Yang, W. Tan, Design of aptamer-based sensing platform using triple-helix molecular switch, Anal. Chem. 83 (2011) 6586-6592.

[21] J. Chen, S. Chen, F. Li, Instrument-free visual detection of tetracycline on an autocatalytic DNA machine using a caged G-quadruplex as the signal reporter, Chem. Commun. 53 (2017) 8743-8746.

[22] Y. Sato, S. Nishizawa, K. Yoshimoto, T. Seino, T. Ichihashi, K. Morita, N. Teramae, Influence of substituent modifications on the binding of 2-amino-1,8-naphthyridines to cytosine opposite an AP site in DNA duplexes: thermodynamic characterization, Nucleic. Acids. Res. 37 (2009) 1411-1422.

[23] R. Freeman, X. Liu, I. Willner, Amplified multiplexed analysis of DNA by the exonuclease III-catalyzed regeneration of the target DNA in the presence of functionalized semiconductor quantum dots, Nano. Lett. 11 (2011) 4456-4461.

[24] F. Xuan, X. Luo, I.M. Hsing, Ultrasensitive solution-phase electrochemical molecular beacon-based DNA detection with signal amplification by exonuclease III-assisted target recycling, Anal. Chem. 84 (2012) 5216-5220.

[25] X. Zuo, F. Xia, Y. Xiao, K.W. Plaxco, Sensitive and selective amplified fluorescence DNA detection based on exonuclease III-aided target recycling, J. Am. Chem. Soc. 132 (2010) 1816-1818.

[26] Q. Fan, J. Zhao, H. Li, L. Zhu, G.X. Li, Exonuclease III-based and gold nanoparticle-assisted DNA detection with dual signal amplification, Biosens. Bioelectron. 33 (2012) 211-215.

[27] X.Z. Wang, T. Hou, T.T. Lu, F. Li, Autonomous exonuclease III-assisted isothermal cycling signal amplification: A facile and highly sensitive fluorescence DNA glycosylaseactivity assay, Anal. Chem. 86 (2014) 9626-9631.

[28] Y. Sato, A. Honjo, D. Ishikawa, S. Nishizawa, N. Teramae, Fluorescent trimethyl-substituted naphthyridine as a ligand for C-C mismatch detection in CCG trinucleotiderepeats, Chem. Commun. 47 (2011) 5885-5887.

[29] J. Wang, X. Wang, S. Wu, R. Che, P. Luo, C. Meng, Fluorescent trimethyl-substituted naphthyridine as a label-free signal reporter for one-step and highly sensitive fluorescent detection of DNA in serum samples, Biosens. Bioelectron. 87 (2017) 984-990.

[30] K. Yoshimoto, S. Nishizawa, A. Masakazu Minagawa, N. Teramae, Use of abasicsite-containing DNA strands for nucleobase recognition in water, J. Am. Chem. Soc. 125 (2003) 8982-8983.

[31] L. Liu, Q. Yang, J. Lei, N. Xu, H. Ju, DNA-regulated silver nanoclusters for label-free ratiometric fluorescence detection of DNA, Chem. Commun. 50 (2014) 13698-13701.

[32] S. Liu, Y. Wang, C. Zhang, Y. Lin, F. Li, Homogeneous electrochemical aptamer-based ATP assay with signal amplification by exonuclease III assisted target recycling, Chem. Commun. 49 (2013) 2335-2337.

[33] Q. Xu, A. Cao, L. Zhang, C. Zhang, Rapid and label-Free monitoring of exonuclease III-assisted target recycling amplification, Anal. Chem. 84 (2012) 10845-10851.

[34] Z. Yang, A.M. Sismour, S.A. Benner, Nucleoside alpha-thiotriphosphates, polymerases and the exonuclease III analysis of oligonucleotides containing phosphorothioate linkages, Nucleic. Acids. Res. 35 (2007) 3118-3127.

[35] A. Ivask, T. Green, B. Polyak, A. Mor, A. Kahru, M. Virta, R. Marks, Fibre-optic bacterial biosensors and their application for the analysis of bioavailable Hg and As in soils and sediments from aznalcollarmining area in Spain, Biosens. Bioelectron. 22 (2007) 1396-1402.

[36] M. Zaib, A. Saeed, I. Hussain, M.M. Athar, M. Iqbal, Voltammetric detection of As(III) with porphyridium cruentum based modified carbon paste electrode biosensor, Biosens. Bioelectron. 62 (2014) 242-248.

Scheme 1. Schematic illustration of the label-free THMS and fluorescence sensing platform. The catalytic assembly is realized through a series of ATMND/HP1-mediated THMS and Exo III-assisted cascade target recycling amplification.

Fig. 1. Evaluation of the label-free THMS and fluorescence sensing platform. (A) The fluorescence emission spectra under different conditions: (a) 1 μM ATMND, (b) 1 μM THMS+1 mg/L As^{3+}+1 μM ATMND/HP1+Exo III, (c) 1 μM THMS+1 μM ATMND/HP1+Exo III, (d) 1 μM ATMND/HP1, (e) 1 μM THMS+1 μM ATMND/HP1, (f) 1 μM THMS+1 mg/L As^{3+}+1 μM ATMND/HP1, and (g) 1 μM THMS; (B) the PAGE image of the platform. Lanes: (a) 1 μM ATMND/HP1, (b) 1 μM THMS+1 μM ATMND/HP1, (c) 1 μM THMS+1 μM ATMND/ HP1+Exo III, (d) 1 μM THMS+1 mg/L As^{3+}+1 μM ATMND/HP1+Exo III, (e) 1 μM THMS+1 mg/L As^{3+}+1 μM ATMND/HP1, and (f) 1 μM THMS.

Fig. 2. Effect of the molar ratio of HP1 to ATMND on the response of the sensing system. Using a fixed concentration of HP1, the concentration of ATMND was changed to obtain different molar ratio. HP1: 1 μM; As^{3+}: 1 mg/L. Error bars represent the standard deviation of three independent measurements.

Fig. 3. Effect of the stem length of ATMND on the response of the sensing system. (a) 1 μM ABA1, (b) 1 μM ABA2, (c) 1 μM ABA3, and (d) 1 μM ABA4. The solution contains 1 μM STP, 1 μM ATMND/HP1, 1 mg/L As^{3+}, and 50 U Exo III.

Fig. 4. Effect of the concentration of ABA1 on the response of the sensing system. The reaction solution contains 1 μM STP, 1 μM ATMND/HP1, 1 mg/L As^{3+} and 50 U Exo III.

Fig. 5. Effect of the incubation time on the response of the sensing system. The reaction solution contains 2 μM ABA1, 1 μM STP, 1 μM ATMND/HP1, 1 mg/L As^{3+} and 50 U Exo III.

Fig. 6. The fluorescence emission spectra of the label-free THMS and fluorescence sensing

platform of various concentrations of As^{3+}. The solution contains 1 μM THMS (2 μM ABA1 and 1 μM STP), 1 μM ATMND/HP1 and 50 U Exo III. Error bars represent the standard deviation of three independent measurements.

Fig. 7. Selectivity investigation of the constructed biosensor for As^{3+} against other control molecules. The concentration is 10 μg/L for As^{3+} and 100 μg/L for other molecules.

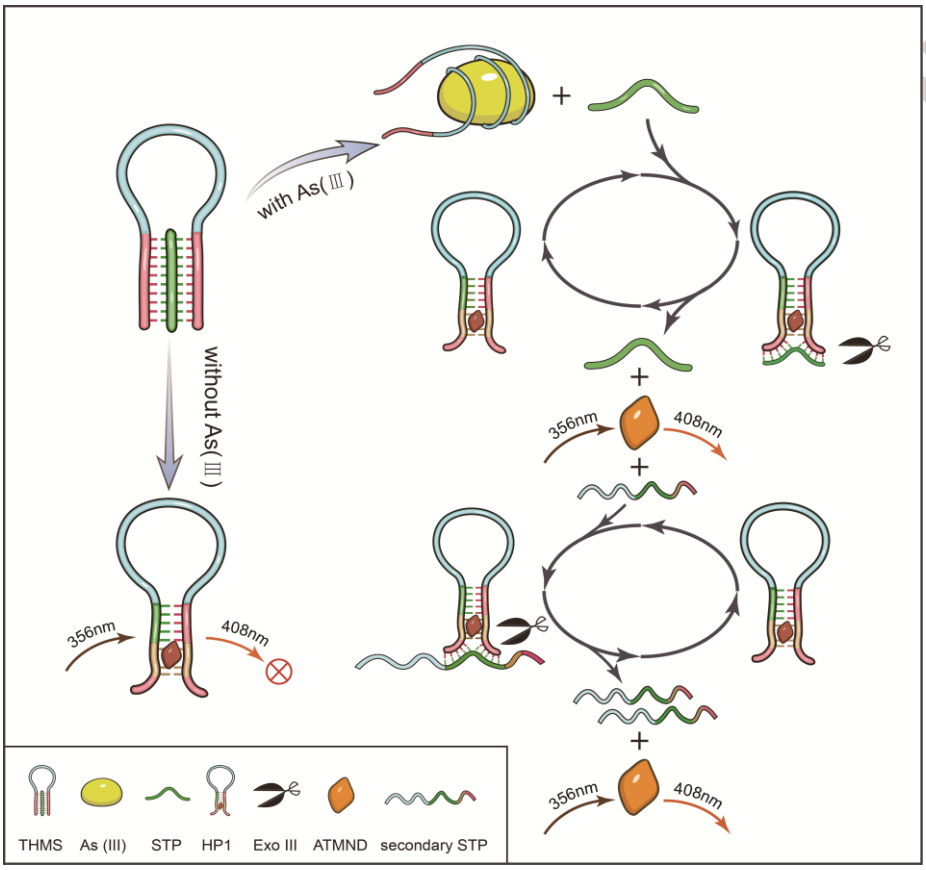

Scheme 1.

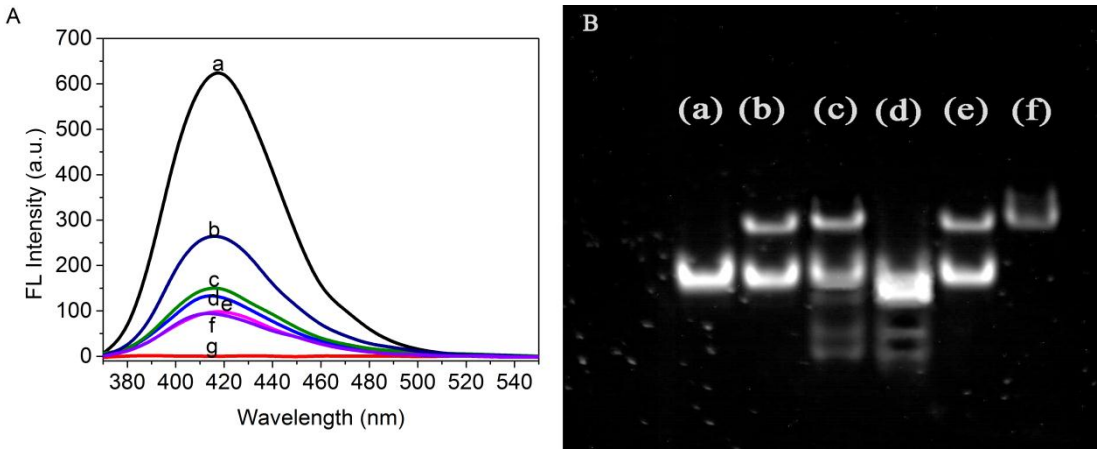

Fig. 1.

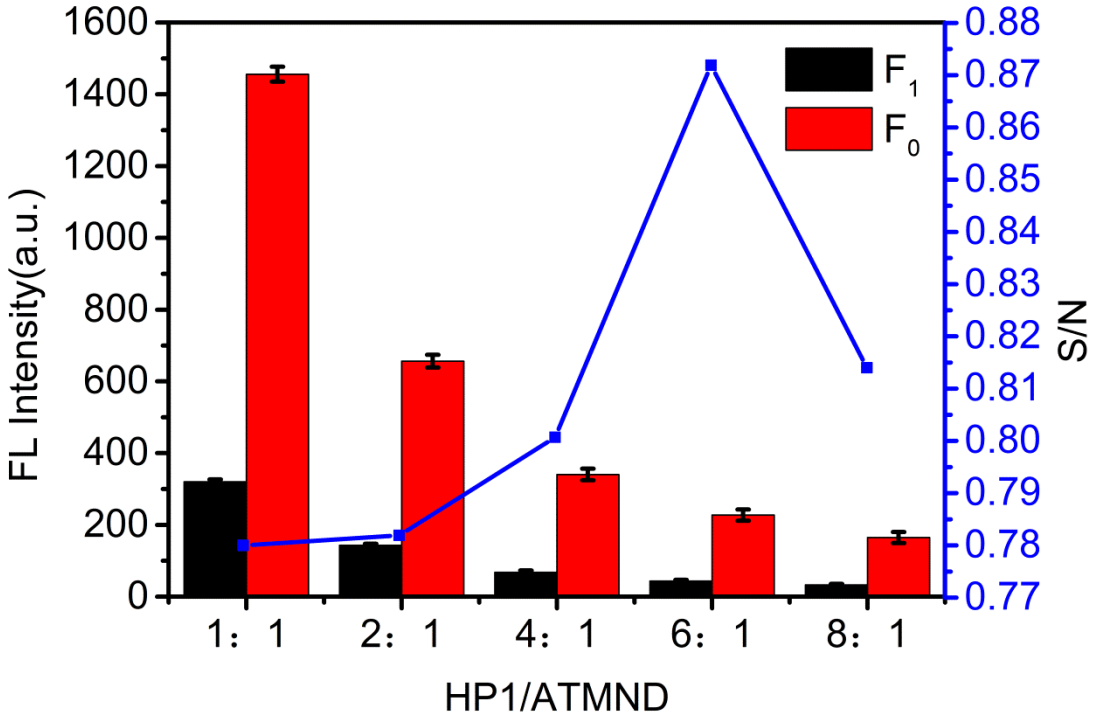

Fig. 2.

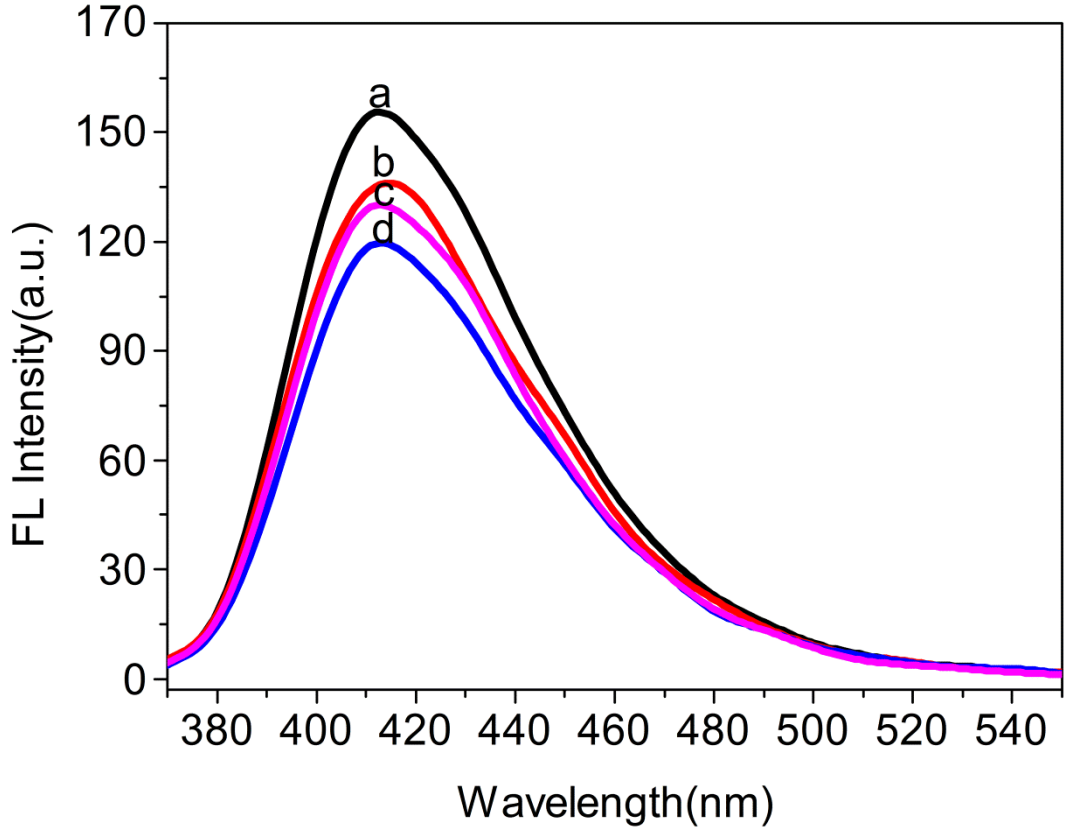
FL Intensity(a.u.)
Wavelength(nm)
a
b
c
d
0
30
60
90
120
150
170
380
400
420
440
460
480
500
520
540

Fig. 3.

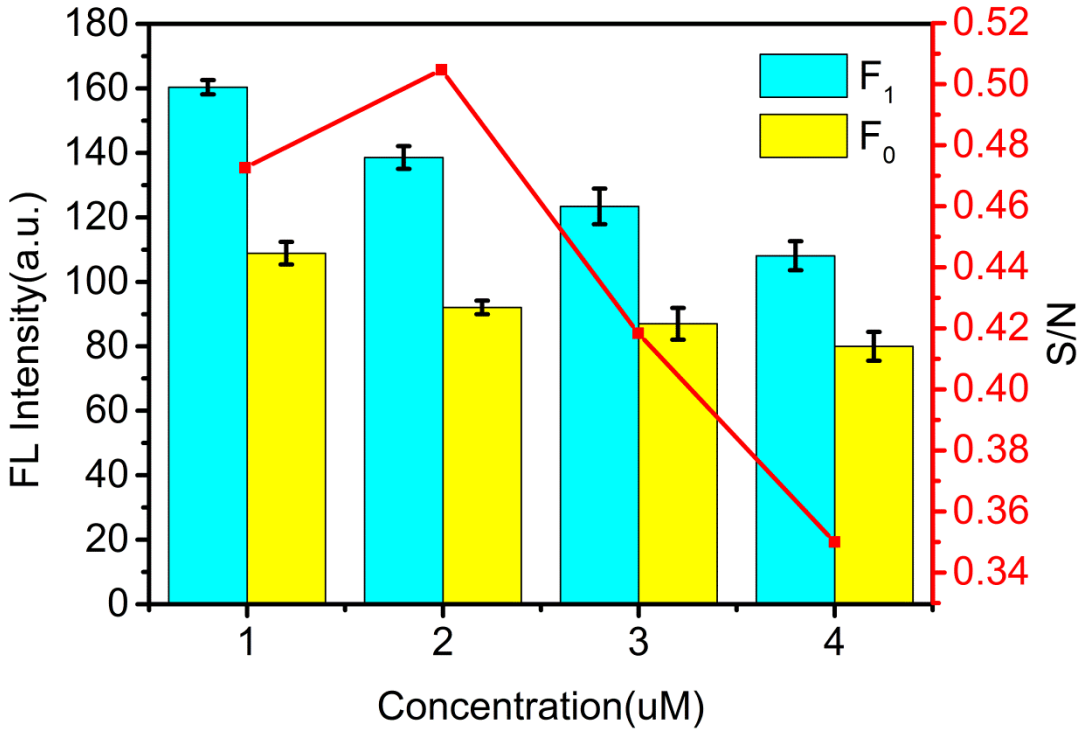
FL Intensity(a.u.)
S/N
Concentration(uM)
F1
F0
0
20
40
60
80
100
120
140
160
180
0.34
0.36
0.38
0.40
0.42
0.44
0.46
0.48
0.50
0.52
1
2
3
4

Fig. 4.

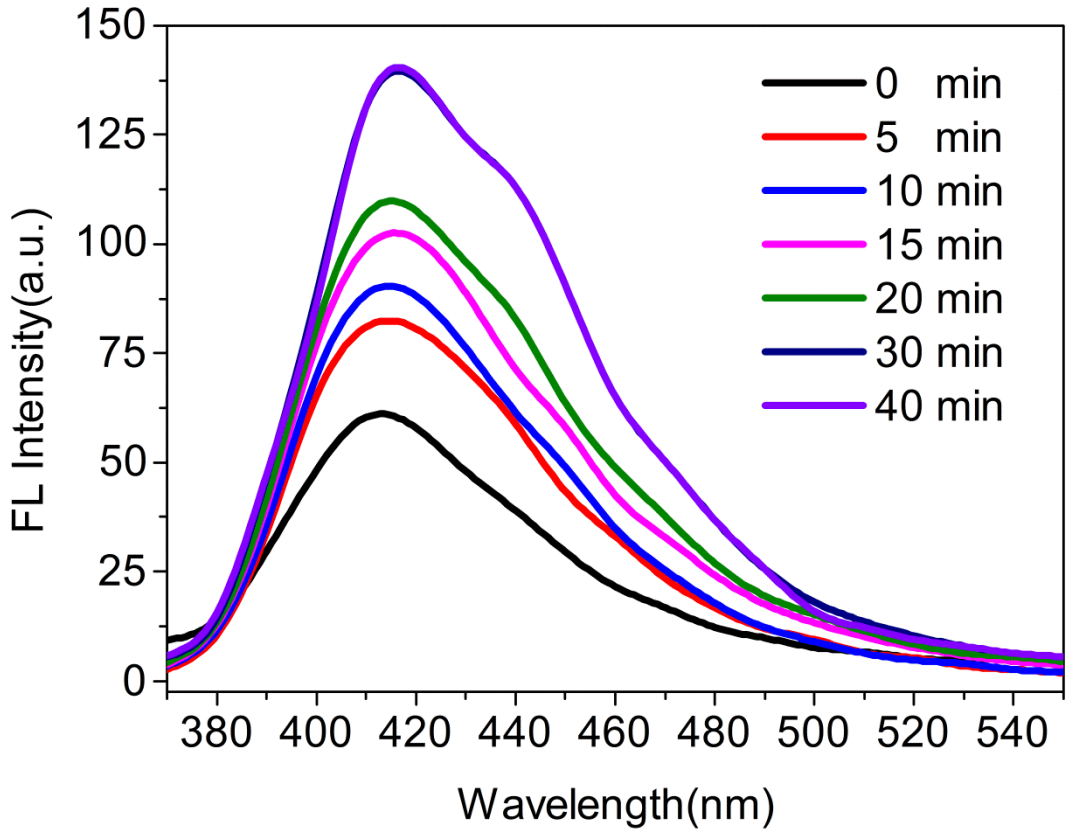
FL Intensity(a.u.)
Wavelength(nm)
0 min
5 min
10 min
15 min
20 min
30 min
40 min

Fig. 5.

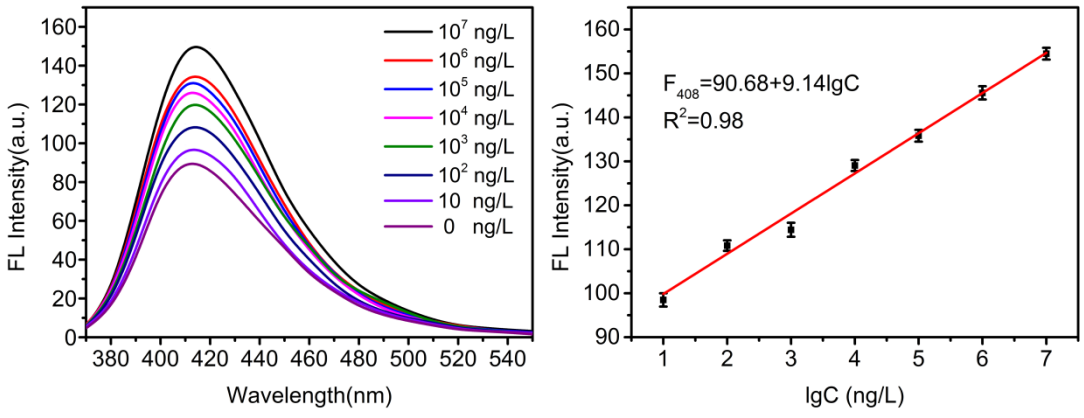
FL Intensity(a.u.)
Wavelength(nm)
10^7 ng/L
10^6 ng/L
10^5 ng/L
10^4 ng/L
10^3 ng/L
10^2 ng/L
10 ng/L
0 ng/L
F408=90.68+9.14lgC
R2=0.98
lgC (ng/L)

Fig. 6.

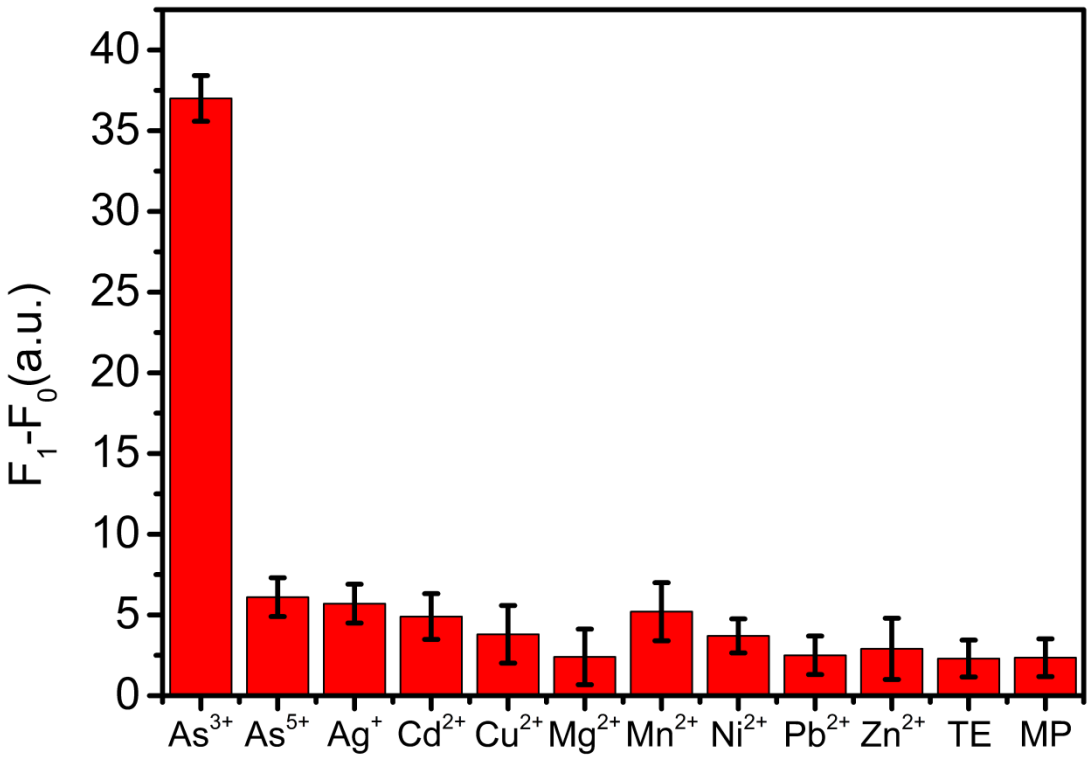

Fig. 7.

Table 1. Application of the label-free fluorescence sensing platform for As^{3+} determination in groundwater.

Sample	Added (μg/L)	Found(mean[a]±SD[b]) (μg/L)	Recovery (%)
1	2.0	2.21 ± 0.12	110.5
2	4.0	4.11 ± 0.23	102.75
3	6.0	6.31 ± 0.33	105.17
4	8.0	7.67 ± 0.49	97
5	10.0	9.79 ± 0.53	97.9

[a]Mean of three determinations. [b]SD, standard deviation.

Table 2. Application of the label-free fluorescence platform for As^{3+} determination in real sample.

Sample	Proposed method[a] (μg/L)	LC-MS/MS[b] (μg/L)	Relative error (Re)[c] (%)
Tap water	0.53 ± 0.05	0.55 ± 0.02	3.64
Lake water	2.21 ± 0.12	2.1 ± 0.08	-5.24
Pond water	4.43 ± 0.22	4.61 ± 0.18	3.90

[a]Each sample was analyzed using our proposed fluorescence sensor, and all values were obtained as an average of three repetitive determinations ± standard deviation (mean ± SD).

[b]Each sample was analyzed using the LC-MS/MS, and all values were obtained as an average of three repetitive determinations ± standard deviation (mean ± SD).

[c]Our proposed method vs. LC-MS/MS.

Highlights:

1. Label-free and sensitive fluorescence detection of As^{3+}.
2. Exonuclease III-assisted signal amplification strategy.
3. The resultingbiosensor was used to detect As^{3+} with a LOD of 5 ng/L and a wider linear range from 10 ng/L to 10 mg/L.
4. The biosensor can be readily expanded to monitor other analytes by substituting the target-specific aptamer sequence.